J Appl Physiol 106: 113–121, 2009.
First published October 30, 2008; doi:10.1152/japplphysiol.00049.2008.

Impairment of coronary flow reserve in aortic stenosis

Damien Garcia,[1] Paolo G. Camici,[2] Louis-Gilles Durand,[3] Kim Rajappan,[2] Emmanuel Gaillard,[3] Ornella E. Rimoldi,[2] and Philippe Pibarot[4]

[1]*Department of Radiology, CRCHUM, University of Montreal Hospital, Montreal, Canada;* [2]*Medical Research Council Clinical Sciences Centre, Hammersmith Hospital, London, United Kingdom;* [3]*Laboratory of Biomedical Engineering, Clinical Research Institute of Montreal, University of Montreal, Montreal, Canada; and* [4]*Quebec Heart Institute, Laval Hospital, Sainte-Foy, Canada*

Submitted 17 January 2008; accepted in final form 21 October 2008

Garcia D, Camici PG, Durand LG, Rajappan K, Gaillard E, Rimoldi OE, Pibarot P. Impairment of coronary flow reserve in aortic stenosis. *J Appl Physiol* 106: 113–121, 2009. First published October 30, 2008; doi:10.1152/japplphysiol.00049.2008.—Coronary flow reserve (CFR) is markedly reduced in patients with severe aortic valve stenosis (AS), but the exact mechanisms underlying this impairment of CFR in AS remain unclear. Reduced CFR is the key mechanism leading to myocardial ischemia symptoms and adverse outcomes in AS patients. The objective of this study was to develop an explicit mathematical model formulated with a limited number of parameters that describes the effect of AS on left coronary inflow patterns and CFR. We combined the mathematical V^3 (ventricular-valvular-vascular) model with a new lumped-parameter model of coronary inflow. One thousand Monte-Carlo computational simulations with AS graded from mild up to very severe were performed within a wide range of physiological conditions. There was a good agreement between the CFR values computed with this new model and those measured in 24 patients with isolated AS ($r = 0.77$, $P < 10^{-4}$). A global sensitivity analysis showed that the valve effective orifice area (EOA) was the major physiological determinant of CFR (total sensitivity index = 0.87). CFR was markedly reduced when AS became severe, i.e., when EOA was <1.0 cm^2, and was generally exhausted when the EOA was <0.5–0.6 cm^2. The reduction of CFR that is associated with AS can be explained by the concomitance of *1*) reduced myocardial supply as a result of decreased coronary perfusion pressure, and *2*) increased myocardial metabolic demand as a result of increased left ventricular workload.

modeling; patients

AORTIC STENOSIS (AS) CREATES an obstruction to blood flow from the left ventricle (LV) to the aorta, which leads to a LV pressure (Plv) overload. The coronary flow reserve (CFR) is defined as the maximal increase in myocardial blood flow (MBF) above its resting level for a given perfusion pressure when coronary vasculature is maximally dilated. The CFR is generally estimated in practice by calculating the ratio of maximum MBF obtained at maximum coronary artery dilation (i.e., hyperemia) induced by pharmacological agents (adenosine, dipyridamole) to resting MBF. This is an integrated measure of flow through both the large epicardial coronary arteries and the microcirculation (23). An abnormal CFR can be due to narrowing of the epicardial coronary arteries or, in the absence of angiographically demonstrable atherosclerotic disease, may reflect dysfunction of the coronary microcirculation. Patients with AS have an impaired CFR, despite normal coronary arteries (21), which limits the ability of coronary circulation to increase flow to match myocardial oxygen demand. The reduction of CFR is the key factor responsible for myocardial ischemia in AS patients, and this may contribute to the development of LV dysfunction, symptoms, and adverse outcomes (34). There still persist some uncertainties and controversies as to the mechanisms underlying the impairment of CFR in AS patients (12). The concentric LV hypertrophy typically associated with AS was initially believed to be the main cause of impaired CFR in these patients (12, 38). Rajappan et al. (34), however, recently reported that CFR correlates better with the hemodynamic indexes of AS severity, i.e., valve effective orifice area (EOA) and transvalvular pressure gradient, than with LV mass. Moreover, in patients with severe AS and no significant obstructive coronary artery disease, ischemic symptoms, such as angina, are generally relieved immediately after aortic valve replacement (AVR), whereas LV hypertrophy gradually regresses over several months. These findings, therefore, suggest that the abnormally high LV workload induced by the stenosis may be one of the key mechanisms responsible for impaired CFR and thus myocardial ischemia in AS.

The objective of this study was to develop an explicit mathematical model formulated with a limited number of independent parameters that describes the effect of AS on left coronary inflow ($\dot{Q}_c$) patterns and CFR. For this purpose, we merged three mathematical models: the V^3 (ventricular-valvular-vascular) model and the analytic expression of the instantaneous maximal transvalvular pressure difference (TPG_{max}) (9, 11), as well as a new lumped-parameter model of $\dot{Q}_c$. The simulated CFR were compared with those measured by Rajappan et al. in a series of patients with AS and normal coronary angiograms (33, 34), whereas the corresponding $\dot{Q}_c$ waveforms were compared with those reported in the literature.

MATERIALS AND METHODS

Mathematical modeling. Three mathematical hemodynamic models were combined. The first model, namely the V^3 model (9), allows one to simulate the waveforms of the Plv, the aortic pressure (Pa), the LV cavity volume, and the cardiac outflow in different physiological and pathophysiological conditions (10). This model consists of the combination of the time-varying elastance model for the LV, the instantaneous pressure-flow relationship for the aortic valve, and the three-element windkessel representation of the peripheral system. The second mathematical model provides the expression of the instantaneous TPG_{max} (11). As the blood flow passes through an AS, it forms a jet, which contracts to a minimum cross-sectional area

Address for reprint requests and other correspondence: D. Garcia, Dept. of Radiology, CRCHUM, 2099 Alexandre de Sève, Montreal, Quebec H2L 2W5, Canada (e-mail: Damien.Garcia@crchum.qc.ca).

The costs of publication of this article were defrayed in part by the payment of page charges. The article must therefore be hereby marked "*advertisement*" in accordance with 18 U.S.C. Section 1734 solely to indicate this fact.

(EOA; see Fig. 1) at the level of the vena contracta. TPG_{max} represents the difference between Plv and the static pressure in the vena contracta. The vena contracta and the left coronary inlet are located at the same distance downstream of the valve annulus (Fig. 1), and it has been shown that the static pressure does not change significantly from the flow axis to the wall (48). The static pressure in the left coronary inlet (P_{inlet}) is thus similar to that in the vena contracta during ejection, so that:

$$\begin{cases} P_{inlet}(t) = Plv(t) - TPG_{max}(t) & \text{during ejection} \\ P_{inlet}(t) = Pa(t) & \text{otherwise} \end{cases} \quad (1)$$

As an example, Fig. 2 shows the pressure waveforms given by the two aforementioned models with a native aortic valve (*top*) or a very severe AS (EOA = 0.4 cm^2, *bottom*), both under normal flow conditions. Finally, the third model consists of a new lumped-parameter representation of the inflow in the left anterior descending (LAD) coronary vessel (see below).

Pressure waveforms. The V^3 model is mainly described by 10 independent cardiovascular parameters (9, 10). The values of these parameters were chosen among typical mean values reported by other investigators (see Table 1). Pressure and cardiac outflow waveforms were simulated with AS varying from nonexistent to very severe, i.e., EOA ranged from 4.0 cm^2 down to 0.3 cm^2. Every simulation was performed using Matlab (The MathWorks). Systole was defined as the period between the onset of the Plv upstroke and the end of ejection. Knowing the cardiac outflow and the Plv and Pa, the P_{inlet} was then calculated by means of the TPG_{max} expression and *Eq. 1*. Finally, the instantaneous LAD $\dot{Q}_c$ was estimated as explained below.

LAD inflow. The left coronary vessel topology was considered as a repetitive network of *N* arbitrary individual layers, distributed in parallel from the epicardium to the endocardium. An electric analog of such a network is illustrated in Fig. 3. One single layer was characterized by a resistor (r_c) in parallel with a capacitor (c_c) with different electrical potential outputs to model the coronary vascular compliance and arteriolar resistance (Fig. 3). As suggested by Holenstein and Nerem (17), the flow within the compliant coronary vessels was assumed to be only a function of the transmural pressure difference

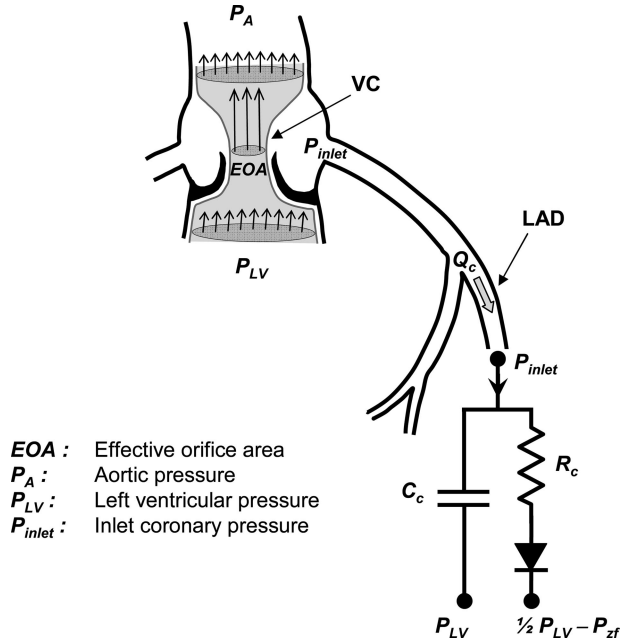

Fig. 1. Schematic representation of the complete mathematical model. VC, vena contracta; LAD, left anterior descending coronary artery, $\dot{Q}_c$, instantaneous LAD blood inflow; C_c, total coronary compliance; R_c, total coronary resistance; P_{zf}, zero-flow pressure.

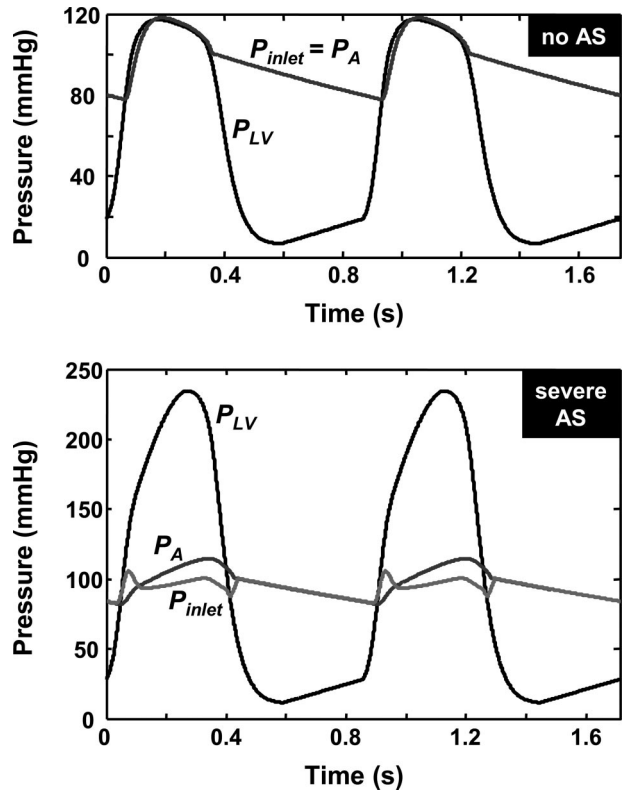

Fig. 2. *Top*: simulated left ventricular (LV) and aortic pressure waveforms with native aortic valve and normal flow conditions. *Bottom*: simulated pressure waveforms with a very severe aortic stenosis (AS) (EOA = 0.4 cm^2) and normal flow conditions. These curves were obtained with the V^3 (ventricular-valvular-vascular) model (9).

(P_{inlet} − IMP_i), where IMP represents the intramyocardial tissue pressure. In the arteriolar resistance, the flow was driven by the difference between the LAD P_{inlet} and the venular pressure (Pv). Both IMP and Pv were supposed to be linearly related to the depth within the LV wall, being proportional to the LV cavity pressure (Plv) in the subendocardium and being equal to zero in the subepicardium. In the

Table 1. *Numerical values of the input cardiovascular parameters implemented in the theoretical model*

	Mean	SD	Reference No.
Left ventricular parameters			
Heart rate, beats/min	69	9	18
Stroke volume, ml	74	15	49
Ejection fraction, %	66	6.6	39
Unloaded volume, ml	−15	30	9
Vascular parameters			
Vascular resistance, mmHg·s·ml^{-1}	0.93	0.17	49
Arterial compliance, ml/mmHg	2.1	0.84	49
STJ aortic area, cm^2	7	3.4	11
LVOT area, cm^2	3.6	0.8	11
Venous pressure, mmHg	5	0.5	9
Coronary parameters			
Zero-flow pressure, mmHg	22	7	31
Normal LAD flow*, ml/min	55	9	18
Normal flow reserve	3.3	0.3	35

Values were obtained in a series of patients with aortic stenosis and normal left ventricular systolic function. STJ, sinotubular junction; LVOT, left ventricular outflow tract; LAD, left anterior descending. *See APPENDIX B.

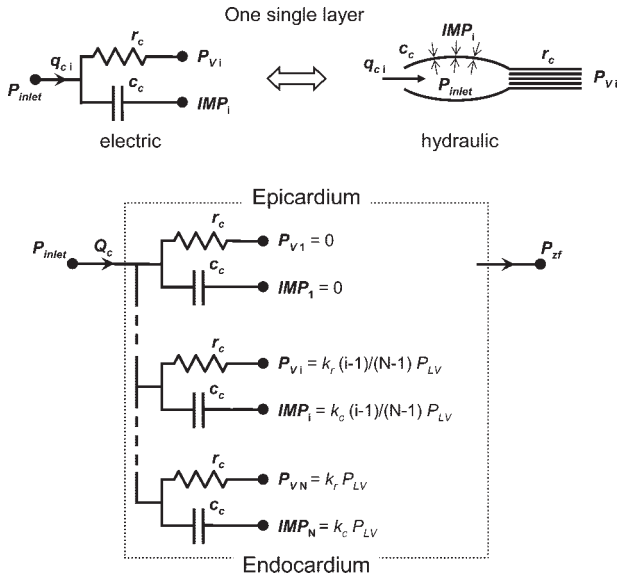

Fig. 3. Schematic illustration of the lumped-parameter coronary inflow model. See the text for symbols and abbreviations.

layer numbered i, IMP_i and Pv_i were thus written as follows: $Pv_i = k_r\,(i-1)/(N-1)\,Plv$ and $IMP_i = k_c\,(i-1)/(N-1)\,Plv$, where k_r and k_c are two constants. An electrical potential was added at the output of the network to simulate the effect of the so-called zero-flow pressure (P_{zf}) (31). Postulating that the resistor and capacitor units are independent of the depth, the contribution of the overall layers yields (see APPENDIX A) the LAD coronary flow:

$$\dot{Q}_c = \frac{1}{R_c}\left(P_{inlet} - 0.5k_rPlv - P_{zf}\right) + C_c\frac{\partial}{\partial t}(P_{inlet} - 0.5k_cPlv) \quad (2)$$

where R_c and C_c represent the functional intramyocardial resistance and compliance, respectively. Because the effect of the Plv on the IMP and the Pv remains poorly understood, it is difficult to assign definite values to k_r and k_c. To be consistent with the resistive branch of the theoretical model developed by Judd and Mates (20), we postulated that $k_r = 1$. Previous studies have also suggested that the IMP in the beating heart is directly related to the Plv at peak systole, but with a IMP-to-Plv ratio varying from 1 to 3, depending on the studies (13, 44). More importantly, the IMP is known to depend also upon the myocardial stiffness, which becomes significant during isovolumic contraction and in late ejection (26, 40). We, therefore, arbitrarily chose $k_c = 2$ to intensify the effect of the LV isovolumic contraction and relaxation on the capacitive LAD flow. Finally, an ideal diode was added to prevent backflow from the venous side as first proposed by Downey and Kick (8). Hence, *Eq. 2* becomes:

$$\dot{Q}_c = \frac{1}{R_c}\overline{R(P_{inlet} - 0.5Plv - P_{zf})} + C_c\frac{\partial}{\partial t}(P_{inlet} - Plv) \quad (3)$$

where the function R is the ramp function [i.e., $R(x) = x$, if $x > 0$, $= 0$ otherwise], which simulates the effect of the diode. The final electric analog model described by *Eq. 3* is depicted in Fig. 1. The P_{zf} and the total coronary compliance C_c have been shown to be relatively independent of the afterload with vasomotor tone intact (20). These two parameters were, therefore, kept constant in our study. A typical value of 22 mmHg was chosen for P_{zf}, as measured in humans during long diastole (31), whereas C_c was fixed at 4×10^{-4} ml/mmHg (see APPENDIX B for details). Integrating *Eq. 3* over one complete cardiac cycle eliminates the capacitive flow and yields the mean LAD blood flow:

$$CBF = \frac{1}{R_c}\overline{R(P_{inlet} - 0.5Plv - P_{zf})} \quad (4)$$

where the overbar denotes the average over the cardiac period, and CBF is coronary blood flow.

$\dot{Q}_c$ waveforms. When LV workload increases, as may occur with AS, myocardial oxygen consumption increases (45) and the metabolic regulation causes arteriolar dilation, leading to a reduction of the arteriolar resistance R_c. This results in an increase in basal CBF (15, 16). CBF is linearly coupled to myocardial oxygen demand (3, 25), which is, in turn, linearly related to pressure-volume area (PVA) and maximal elastance (E_{max}) (46). Thus the ratio of CBF to mean CBF in the absence of AS (CBF_{noAS}) can be written as:

$$\frac{CBF}{CBF_{noAS}} = \frac{aPVA + bE_{max} + c}{aPVA_{noAS} + bE_{max_{noAS}} + c} \quad (5)$$

where PVA_{noAS} (= 1.4 J) and $E_{max_{noAS}}$ (= 1.6 mmHg/ml) were calculated from the waveforms obtained without AS (see APPENDIX B), while the coefficients a, b, and c were issued from Suga (45). From *Eqs. 4* and *5*, R_c can finally be written as:

$$R_c = \left(\frac{aPVA_{noAS} + bE_{max_{noAS}} + c}{aPVA + bE_{max} + c}\right)\frac{\overline{R(P_{inlet} - 0.5Plv - P_{zf})}}{CBF_{noAS}} \quad (6)$$

where CBF_{noAS} = 55 ml/min (see APPENDIX B). For every simulated condition, R_c was calculated from *Eq. 6*, and $\dot{Q}_c$ was computed using *Eq. 3*.

CFR. CFR reflects the maximal coronary flow capacity and is defined as the ratio of maximal hyperemic flow to basal resting flow. Hyperemic flow is obtained in practice when coronary arteriolar vasculature is maximally dilated by pharmacological stressors (as dipyridamole or adenosine), i.e., when R_c is minimal. CFR can be estimated either by using positron emission tomography (23) or by catheterization with a Doppler flow wire (15). It has been shown that dipyridamole and adenosine have no or minimal effects on the other hemodynamic parameters (systemic arterial compliance and resistance, cardiac output, etc.). Using *Eq. 4*, CFR can thus be written as a function of the coronary resistance:

$$CFR = \frac{CBF_{hyperemia}}{CBF} = \frac{R_c}{R_{c\,hyperemia}} \quad (7)$$

where $CBF_{hyperemia}$ is hyperemic CBF. Assuming now that $R_{c\,hyperemia}$ (minimal R_c) remains unchanged in the same patient during the progress of AS, one may write:

$$CFR = \frac{R_c}{R_{c\,noAS}}CFR_{noAS} \quad (8)$$

where CFR_{noAS} is the CFR without AS whose value was fixed at 3.3 (35), and $R_{c\,noAS}$ is R_c without AS. CFR was estimated for every simulated condition by combining *Eqs. 6* and *8*. These two equations show that CFR is directly dependent on the coronary perfusion pressure ($P_{inlet} - 0.5\,Plv - P_{zf}$) and the metabolic demand characterized by the PVA and E_{max}.

Numerical simulations and sensitivity analysis. To study how the theoretical CFR is affected by hemodynamic conditions (heart rate, stroke volume, systemic resistance and compliance, etc.), a sensitivity analysis was performed by running 1,000 Monte-Carlo simulations (*study 1*), representing 1,000 hypothetical patients with mild to very severe AS within a wide range of physiological conditions. The values of each input parameter, except EOA, were randomly allocated from normal distributions with mean and standard deviation values reported in the literature (see Table 1). For example, stroke volume was randomly drawn from a normal distribution with mean 74 ml and standard deviation 15 ml (Table 1). Random EOA values were drawn from a uniform distribution on the interval 0.3–2.0 cm^2. A global sensitivity analysis (36) was then performed to further analyze the

involvement of EOA in CFR. The first order and total sensitivity indexes for EOA were calculated using a general variance decomposition scheme (42). The first-order sensitivity index denotes the relative importance of EOA in driving the uncertainty on CFR, while the total sensitivity index relates the importance of EOA in combination with other input variables. Five supplementary series of 100 Monte-Carlo simulations each were also run with respective EOA values of 0.5, 1, 1.5, 2, and 4 cm^2 (*study 2*) to further analyze the impact of AS severity on CFR.

Comparison with in vivo data. To validate our theoretical model, we compared the simulated CFR with those measured in 24 patients with isolated moderate to severe AS and angiographically normal coronary arteries. Patients' characteristics and methods were described in detail by Rajappan et al. (34). Briefly, EOA was measured by transthoracic Doppler-echocardiography using the continuity equation. The MBF was measured by oxygen-15-labeled water and positron emission tomography scan at rest and at hyperemia, induced by injection of dipyridamole (0.56 mg/kg). CFR was calculated as the ratio of hyperemic MBF to resting MBF (23).

Statistical analysis. The series (EOA, CFR) issued from the 1,000 simulations (*study 1*) were fitted in a total least squares sense with a function f(EOA) defined by $f(\text{EOA}) = a - b\exp(-c\,\text{EOA})$, where a denotes CFR without AS. Goodness of fit was determined by measuring the Pearson correlation coefficient between simulated and fitted CFR. CFR data measured in patients with AS were compared with CFR predicted by the fitting equation ($n = 24$) by means of the correlation coefficient and a Bland-Altman plot: (predicted − measured) vs. 1/2 (predicted + measured). The five CFR groups issued from *study 2* were compared using a Tukey multiple-comparison test. A notched box-and-whisker plot was also used to summarize these five data series (1).

RESULTS

Coronary flow waveforms. The findings are consistent with the data previously reported in normal subjects (Fig. 4), as well as in AS patients after AVR (14, 19, 24, 51). In the absence of AS, the inlet coronary flow depicts a typical biphasic pattern (Fig. 4, *top*) and the systolic CBF (S) represents ~25% of total CBF (S+D). In the presence of AS, the systolic CBF decreases with increasing stenosis severity due to the marked increase in LV IMP during systole. The systolic CBF becomes close to zero when the valve EOA decreases below 0.5–0.6 cm^2 (Fig. 5, *top*). Moreover, when AS is very severe (e.g., EOA = 0.4 cm^2, Fig. 5, *top*, and Fig. 4, *bottom*), a retrograde flow appears during systole, as reported in previous studies (4, 14, 18, 24, 32), and CBF essentially occurs during diastole. It should be noted that the LAD flow simulated in conditions of severe AS is very similar (Fig. 4, *bottom*) to that previously reported in patients with severe AS (14, 18, 32). Figure 5 (*top*) shows that diastolic CBF increases markedly when EOA decreases. Indeed, as AS severity increases, total (diastolic and systolic) resting CBF raises to match the increase in myocardial demand associated with the rise in LV workload (Fig. 6). On the other hand, the hyperemic CBF is reduced because the driving pressure ($P_{inlet} - 0.5\,Plv - P_{zf}$) governing the coronary perfusion and thus the myocardial supply decreases with increasing stenosis severity (Fig. 6). These two mechanisms both contribute to the impairment of CFR that is typically observed in the presence of AS. The simulations also illustrate that AS does not significantly alter the diastolic coronary flow during hyperemia, whereas the systolic flow vanishes and turns out to be negative as AS becomes severe (Fig. 5, *bottom*).

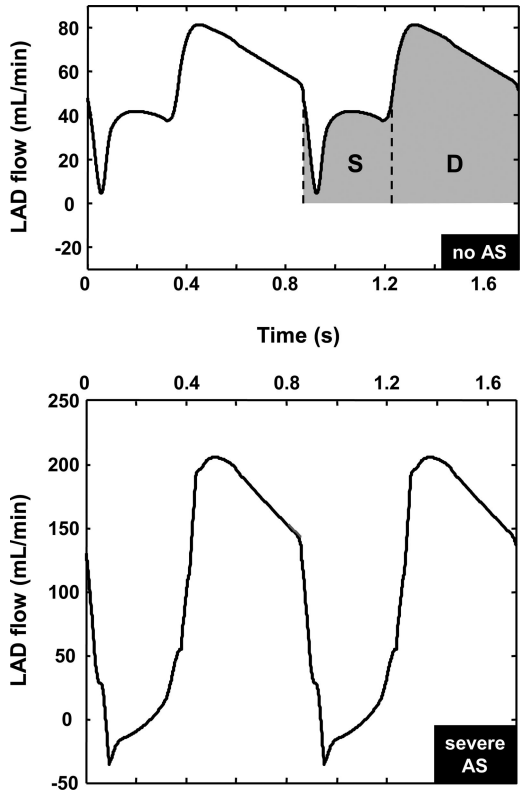

Fig. 4. *Top*: simulated LAD inflow without AS (see the corresponding Fig. 2, *top*). S, flow-time integral during systole; D, flow-time integral during diastole. *Bottom*: simulated LAD inflow with severe AS (EOA = 0.4 cm^2, see the corresponding Fig. 2, *bottom*). These simulations are very consistent with coronary velocity waveforms reported in the literature with native valve [see Fig. 4 from Hozumi et al. (19)] and AS [see Fig. 2 from Hongo et al. (18)].

CFR. CFR was highly dependent upon EOA (Fig. 7). The scatter plot shows that the mathematical model for estimating CFR remained robust, despite the large ranges used for the input parameters (Fig. 7). The global sensitivity analysis reported a value of 0.87 for first-order and global sensitivity indexes of EOA. Because there was no interaction between input variables in our model, the respective sums of all first-order and global indexes are equal to 1. This means that the other input variables (heart rate, ejection fraction, stroke volume, etc., see Table 1) have little effect on CFR, despite the large hemodynamic setting. The fitting curve [$\text{CFR} = 3.30 - 4.21\exp(-1.76\,\text{EOA})$, $r = 0.92$, $P < 10^{-9}$] shows that CFR decreases exponentially with decreasing EOA (Fig. 7). A satisfactory correlation was observed between CFR measured in patients and those predicted by the fitting equation ($r = 0.77$, $P < 10^{-4}$). Their difference was, on average, −0.03 (SD = 0.38), which supports the validity of the theoretical model (Fig. 8). The results issued from *study 2* are summarized on the box-and-whisker plot (Fig. 9). CFR decreases rapidly when EOA becomes <1.5 cm^2 (cutoff value generally used for the definition of moderate AS). The multiple-comparison test showed that all of the groups have CFR means significantly different from each other ($P < 10^{-4}$). CFR medians (estimated 95% confidence intervals) are 1.53 (1.48–1.58), 2.64 (2.58–2.71), 2.98 (2.91–3.04), 3.18 (3.13–3.23), and 3.42 (3.35–3.48) for EOA = 0.5, 1, 1.5, 2, and 4 cm^2, respectively (Fig. 9).

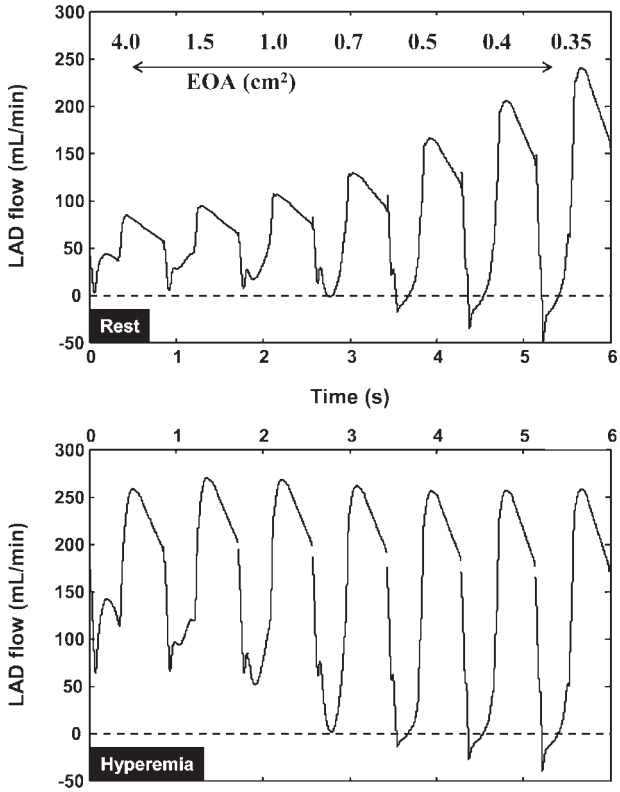

Fig. 5. Simulated LAD inflows from nonexistent to very severe AS, at rest (*top*) and under pharmacologically induced hyperemia (*bottom*).

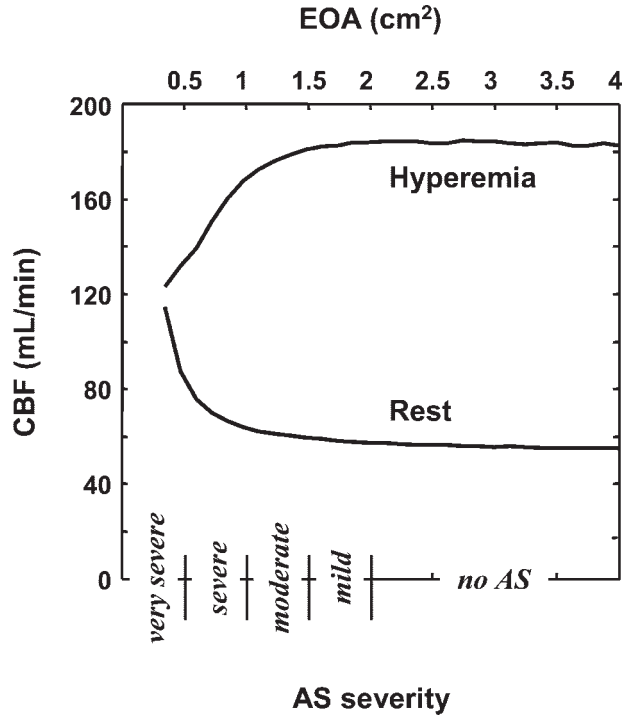

Fig. 6. Simulated resting and hyperemic mean coronary blood flows (CBF) as a function of valve EOA.

DISCUSSION

The main contribution of this paper was to develop and validate a new mathematical model that accurately describes the effects of AS on CBF. This model may be helpful to assess the respective contribution of the hemodynamic factors that independently influence the CFR in these patients. In this study, we used this new model to examine the physiological relationship between valve EOA and CFR. The results support the notion that the valve EOA has a direct and profound effect on CFR.

The numerical coronary model. Numerous CBF models have been proposed, from simple lumped-parameter (8, 17, 20, 47) to complex distributed representations (2, 5, 40). Because we only examined the $\dot{Q}_c$, we represented the left coronary arterial vasculature as individual layers whose behavior was characterized by only two parameters, namely, the total arterial compliance and vascular resistance. The final coronary model obtained here is somewhat similar to the one proposed by Judd and Mates (20) and takes account of the pumping action of the cardiac muscle as first proposed by Spaan et al. (43) in their intramyocardial pump model. The only difference with Judd and Mates' model with respect to the resistive flow component lies in the presence of the ramp function influencing the mean systolic $\dot{Q}_c$ in case of abnormally high afterload. With regard to the capacitive component, the flow is regulated by the transmural pressure in our model, whereas it depends only upon the Pa in the Judd and Mates' model. The flow waveforms obtained with this improved model showed a retrograde flow during isovolumic contraction and early ejection, which is consistent with what was previously reported in patients with severe AS (14, 18, 32), as well as in waveforms simulated with the use of complex mathematical models (40, 41).

CBF and reserve in AS. The Plv overload imposed by the stenotic aortic valve triggers the development of concentric LV

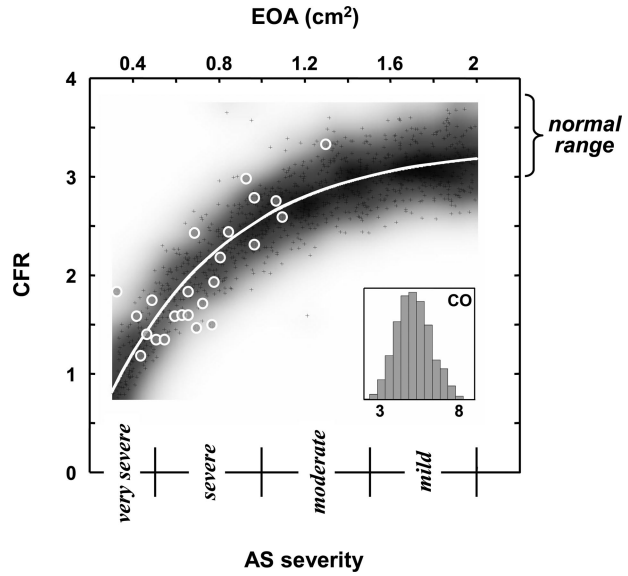

Fig. 7. Scatterplot of the 1,000 Monte-Carlo simulations: computed coronary flow reserve (CFR) as a function of EOA over a large range of input physiological conditions (see Table 1 and text). The shaded area represents the smoothed scatter plot of the results around the fitting curve (white line). The white circles illustrate the patients' data (n = 24). The "normal range" refers to the coronary flow reserve in normal subjects. The *inset* depicts the histogram related to cardiac output (CO; in l/min) and illustrates the wide hemodynamic conditions over the 1,000 simulations. Estimated mean and SD for cardiac output are 5.14 and 1.08 l/min, respectively.

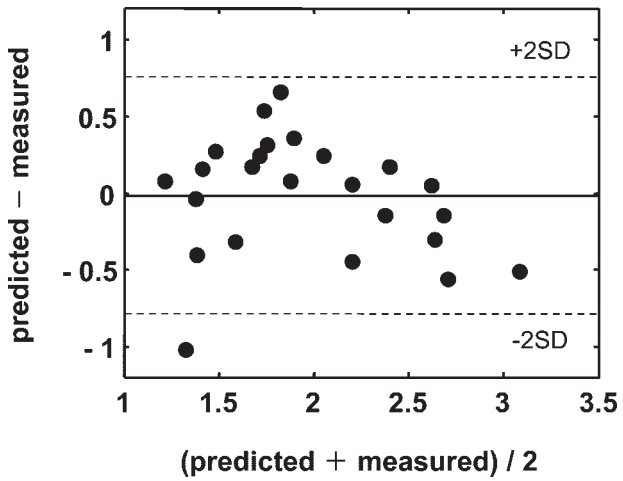

Fig. 8. Bland-Altman plot showing comparison between CFR measured in patients and that predicted by the fitting equation.

hypertrophy. Total CBF increases in relation to LV mass, whereas arteriolar density is reduced. The combination of these two abnormalities may contribute to the reduction of the autoregulatory capacity of the coronary microcirculation in patients with LV concentric hypertrophy associated with AS. This mechanism was believed to be the main cause of impaired CFR in AS patients. This hypothesis, however, has been challenged by the study of Rajappan et al. (34), which revealed that CFR is more strongly related to the hemodynamic severity of valve stenosis rather than to LV mass. In this previous study, including patients with AS and angiographically normal coronary arteries, CFR correlated well with valve EOA, whereas there was only a weak correlation with LV mass. In line with these previous clinical data, the results of this study support the concept that the stenosis severity, as documented by the valve EOA, is an important physiological determinant of CFR. From the $\dot{Q}_c$ model developed and validated in the present study, it was indeed demonstrated that the CFR rapidly drops when EOA becomes <1.0 cm^2 (Figs. 7 and 9). For EOA values smaller than 0.5–0.6 cm^2, the CFR is close or equal to 1.0, indicating limited or no ability to increase CBF in response to increased metabolic demand (Figs. 7 and 9). Such level of CFR may expose the myocardium to repetitive ischemia, which, in turn, induces a progressive loss of contractile material within the myocytes, leading to the development of LV dysfunction. The myocardial ischemia associated with exhaustion of CFR is also believed to be the main mechanism responsible for the occurrence of angina pectoris and potentially fatal arrhythmias that may be observed in AS patients, even if they have angiographically normal epicardial coronary arteries (21). In turn, angina is associated with a marked increase in the risk of sudden death in AS patients (27). These findings underline that the normalization of CFR is a crucial objective of AVR. To this effect, it is interesting to note that angina and ECG signs of myocardial ischemia are often relieved immediately after AVR, whereas regression of LV hypertrophy may occur over the next several months or years after operation (30). Moreover, Rajappan et al. (34) reported that changes in CFR after AVR in patients with severe AS and normal coronary angiograms were directly dependent on change in valve EOA achieved with AVR. These findings are consistent with the results of the present study showing that, beyond LV hypertrophy, the hemodynamic severity of the stenosis, as reflected by reduced valve EOA, is a major determinant of CFR impairment in AS.

As reflected by the increase in PVA and E_{max}, LV workload and thus myocardial oxygen consumption increase as a result of increased LV intracavitory pressure. Consequently, the basal CBF increases to match this increased myocardial demand (Fig. 6). Moreover, the augmentation in the LV intracavitory pressure translates into a decrease in the coronary perfusion pressure, which limits the ability of the coronary circulation to increase CBF in response to the increased myocardial demand. In the presence of very severe AS, the high systolic IMP even induces a systolic reversal CBF. These factors may all contribute to limit the myocardial blood supply. Hence, as depicted by *Eqs. 6* and *8*, the reduction of CFR that is associated with AS can be explained in large part by the concomitance of *1*) reduced myocardial supply as a result of decreased coronary perfusion pressure and diastolic duration; and *2*) increased myocardial metabolic demand as a result of Plv overload. The increased myocardial demand is essentially reflected by an increase in the resting CBF, whereas the reduced supply is reflected by a decrease in the maximal (hyperemic) CBF (Fig. 6).

Potential clinical implications and further investigations. The clinical approach usually requires the realization of a large number of physiological measurements in a large cohort of subjects, and these measurements may often be difficult or

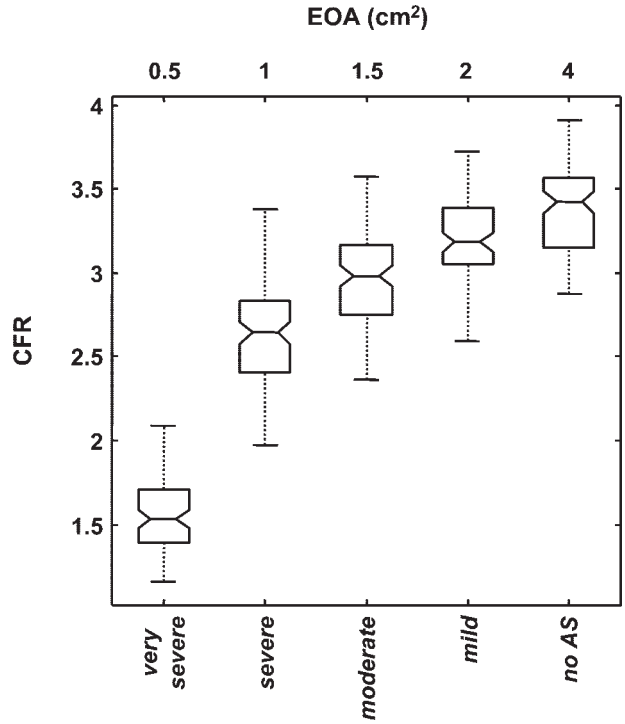

Fig. 9. Box-and-whisker plot showing the simulated CFR for different AS grades (*study 2*). The *top* and *bottom* of each box represent the 25th and 75th percentiles of the samples, respectively. The line in the *middle* is the sample median. The whiskers represent the highest and lowest observations. Notches display the variability of the median between samples: box plots whose notches do not overlap (as in this figure) have different medians at the 5% significance level.

even impossible to perform in patients. The utilization of computational methods may overcome the difficulty in performing a comprehensive analysis of the interaction between different physiological systems. In the present study, we showed that a combination of simple mathematical models may shed some light on a physiological phenomenon as complex as the impairment of CBF in the presence of AS. The results of this study may have important clinical implications.

The guidelines of the American College of Cardiology-American Heart Association suggest that AVR is recommended when the stenosis is severe and the patient has symptoms. Hence, the presence of a severe stenosis in the absence of symptoms is not considered as a class I indication for AVR. The main limitation of this approach is that the identification of symptoms may be difficult, especially in the elderly patients who represent the vast majority of the AS population. The results of the present study suggest that an EOA $< 0.5–0.6$ cm^2 is an indicator for markedly reduced CFR, which may substantially increase the risk of myocardial ischemia, LV dysfunction, or sudden death. Hence, such a level of EOA should alert the clinician, even if the patient claims to be asymptomatic. Exercise testing, exercise stress echocardiography, and dosage of plasma natriuretic peptides should be considered in this situation to corroborate the disease severity and confirm or infirm the indication of AVR. Our findings also provide some support in favor of raising the level of indication (currently IIb) for AVR in the case of very severe AS (EOA < 0.6 cm^2) in asymptomatic patients. However, such change in the guidelines needs to be buttressed by more studies corroborating these findings and confirming the independent impact of hemodynamic stenosis severity on other clinical outcomes. To this effect, a recent study by Mihaljevic et al. (29) reported that the preoperative valve EOA is a powerful independent predictor of late survival after AVR after adjustment for other risk factors, including age, LV mass, and LV ejection fraction. They also reported that severe LV hypertrophy has a negative impact on survival, independently of valve EOA. For a given degree of stenosis severity and therefore a given level of Plv overload, the magnitude and pattern of LV hypertrophy may vary extensively from one patient to another, depending on age, sex, chronicity of AS, concomitant diseases, and genetic factors. Besides of its negative effect on CFR, LV hypertrophy may also predispose to the development of LV diastolic and systolic dysfunction. The normalization of LV mass and associated abnormalities is often incomplete after valve replacement, thus explaining the reduction in postoperative survival independently associated with severe LV hypertrophy.

Assumptions and limitations of the LAD flow model. To obtain a simplified expression of the LAD inflow, we hypothesized that r_c is uniform within the myocardium, i.e., that the resistance distribution is homogeneous throughout the LV wall layers. This is possibly true at the level of the arterioles, where the diameter is mainly controlled by the coronary autoregulation. For larger arteries, however, the transmural pressure affects the cross-sectional area (16) and thus the hydraulic resistance. Because ~25% of total resistance occurs in coronary arteries under normal conditions (6), one may, therefore, expect that the resistance distribution is heterogeneous throughout the LV depth and changes through the cardiac cycle. Some complex models of the coronary circulation integrate the space and time dependence of the vessel properties (2, 41), which may provide more complete information, such as the spatial and temporal distribution of the CBFs. Since we exclusively focused on the LAD inflow, such a model would have been unnecessarily too complex for the purpose of the present study. Although a lumped-parameter model has a limited anatomical representation, it may describe adequately one specific physiological aspect with a restricted number of parameters. Another assumption was required to complete the calculation of CFR (see *Eqs. 7* and *8*): the hyperemic coronary resistance was assumed to be independent of the AS severity. As AS progresses, the subsequent pressure overload induces the development of LV hypertrophy as also observed with systemic arterial hypertension. However, as opposed to what is observed in patients with arterial hypertension, there is no wall thickening of intramyocardial arterioles in those with AS (37), which supports that extravascular mechanisms, rather than vessel structural or functional alterations, are responsible for the CFR reduction in the AS patients (34). Despite these aforementioned limitations, we observed a very good concordance between the computational findings and the measurements performed in patients. Our results suggest that the hemodynamic load imposed by the stenosis is a major determinant of CFR impairment in AS patients. It should be noted that the model, however, does not allow the determination of the precise independent contribution of other factors that may influence the myocardial oxygen consumption and/or delivery and thereby the CFR, including LV hypertrophy, coronary artery disease, and hypertension.

Conclusion. The numerical model developed in the present study accurately simulated the coronary flow waveforms and CFRs observed in normal subjects, as well as in patients with AS. The simulations obtained with this model showed that the valve EOA is one of the main physiological determinants of CFR. CFR is markedly reduced when AS becomes severe, i.e., EOA is <1.0 cm^2, and is generally exhausted when the EOA is $<0.5–0.6$ cm^2. Operative strategies aiming at implanting the prosthetic valve, providing the largest possible EOA in relation to the patient's size, may contribute to optimize the recovery of CFR after AVR. Further computational and in vivo studies are needed to determine the influence of LV hypertrophy, as well as concomitant diseases, such as systemic arterial hypertension or obstructive coronary artery disease, on CFR of patients with AS.

APPENDIX A: ELECTRIC ANALOG OF THE CORONARY MODEL

One seeks the electric analog of the coronary LAD model depicted in Fig. 3. The inflow $q_{c\,i}$ in one single layer numbered i is given by:

$$q_{c\,i} = \frac{P_{inlet} - Pv_i - P_{zf}}{r_c} + j\omega c_c(P_{inlet} - IMP_i) \qquad (A1)$$

where Pv_i and IMP_i are the respective Pv and IMPs within the layer i, ω is the pulsation frequency, and j is the unit complex number. Pv_i and IMP_i are assumed to be directly proportional to the intracavitory Plv, and their magnitudes are supposed to be linearly related to the depth in the LV wall, equaling zero in the supepicardium ($i = 1$) so that:

$$\mathrm{Pv}_i = k_r \frac{i-1}{N-1}\mathrm{Plv} \quad \text{and} \quad \mathrm{IMP}_i = k_c \frac{i-1}{N-1}\mathrm{Plv} \qquad (A2)$$

where k_r and k_c are two constants, and N is the (arbitrary) total number of layers. Using these expressions, *Eq. A1* thus becomes:

$$q_{c\,i} = \frac{\mathrm{P_{inlet}} - k_r(i-1)/(N-1)\mathrm{Plv} - \mathrm{P_{zf}}}{\mathrm{r_c}} + j\omega \mathrm{c_c}[\mathrm{P_{inlet}} - k_c(i-1)/(N-1)\mathrm{Plv}] \qquad (A3)$$

The LAD $\dot{\mathrm{Q}}_c$ is given by the sum of the individual $q_{c\,i}$ so that:

$$\dot{\mathrm{Q}}_c = \frac{1}{\mathrm{r_c}}\sum_{i=1}^{N}[\mathrm{P_{inlet}} - k_r(i-1)/(N-1)\mathrm{Plv} - \mathrm{P_{zf}}] + j\omega \mathrm{c_c}\sum_{i=1}^{N}[\mathrm{P_{inlet}} - k_c(i-1)/(N-1)\mathrm{Plv}] \qquad (A3)$$

After defining the total resistance and compliance of the LAD downstream network by $\mathrm{R_c} = \mathrm{r_c}/N$ and $\mathrm{C_c} = N \times \mathrm{c_c}$, respectively, *Eq. A3* can be simplified in the time domain ($j\omega$ is changed to $\partial/\partial t$), as follows:

$$\dot{\mathrm{Q}}_c = \frac{1}{\mathrm{R_c}}(\mathrm{P_{inlet}} - 0.5k_r\mathrm{Plv} - \mathrm{P_{zf}}) + \mathrm{C_c}\frac{\partial}{\partial t}(\mathrm{P_{inlet}} - 0.5k_c\mathrm{Plv}) \qquad (A4)$$

Note that the arbitrary N parameter, which represents the total number of layers, does not appear in the final equation (*Eq. A4*).

APPENDIX B: ESTIMATION OF THE CORONARY COMPLIANCE AND OTHER PARAMETERS

Preliminary simulations were performed with a normal aortic valve (EOA = 4.0 $\mathrm{cm^2}$) to adjust $\mathrm{C_c}$, as described hereinafter. The normal mean CBF ($\mathrm{CBF_{noAS}}$) in LAD of control subjects (no AS) has been reported to be around 55 ml/min (18, 50). [Note here that the CBF values provided by Hongo et al. (18) have been divided by two; see APPENDIX C for details.] According to *Eq. 4*, the corresponding coronary resistance without AS is, therefore, $\mathrm{R_{c\,noAS}} = 53\ \mathrm{mmHg \cdot s \cdot ml^{-1}}$. A series of $\dot{\mathrm{Q}}_c$ waveforms was simulated using *Eq. 3* with $\mathrm{R_c} = \mathrm{R_{c\,noAS}}$ and different $\mathrm{C_c}$ values. The suitable value for $\mathrm{C_c}$ was estimated by means of a minimization method so that the ratio of the systolic to diastolic flow-time integral (S/D, see Fig. 4, *top*) was equal to 0.36, as reported in control subjects (18). This yielded $\mathrm{C_c} = 4 \times 10^{-4}$ ml/mmHg. The same simulation also gave $\mathrm{PVA_{noAS}} = 1.4$ J and $\mathrm{E_{max_{noAS}}} = 1.6$ mmHg/ml (see *Eqs. 5* and *6*).

APPENDIX C: WOMERSLEY NUMBER IN THE LAD

The Womersley number α characterizes the unsteady nature of a periodic flow. It is defined as (28):

$$\alpha = \frac{D}{2}\sqrt{\frac{\omega\rho}{\mu}}$$

where D is the vessel diameter, and ω, ρ, and μ are the angular frequency of the flow, the blood density, and the blood dynamic viscosity, respectively. A typical diameter for LAD in adults is 3 mm so that $\alpha \approx 2.5$ with a heart rate of 70 beats/min (i.e., $\omega = 7.3$). Such a low α shows that the viscous effects are predominant over the unsteady effects (28). The velocity profiles are, therefore, mostly parabolic in LAD (22). Because Hongo et al. (18) assumed flat profiles to calculate the blood flow in LAD from the Doppler velocities, their values must be multiplied by 0.5, as recommended by Doucette et al. (7).

REFERENCES

1. **Benjamini Y.** Opening the box of a boxplot. *Am Stat* 42: 257–262, 1988.
2. **Bovendeerd PH, Borsje P, Arts T, van De Vosse FN.** Dependence of intramyocardial pressure and coronary flow on ventricular loading and contractility: a model study. *Ann Biomed Eng* 34: 1833–1845, 2006.
3. **Braunwald E, Sarnoff SJ, Case RB, Stainsby WN, Welch GH Jr.** Hemodynamic determinants of coronary flow: effect of changes in aortic pressure and cardiac output on the relationship between myocardial oxygen consumption and coronary flow. *Am J Physiol* 192: 157–163, 1958.
4. **Carroll RJ, Falsetti HL.** Retrograde coronary artery flow in aortic valve disease. *Circulation* 54: 494–499, 1976.
5. **Chadwick RS, Tedgui A, Michel JB, Ohayon J, Levy BI.** Phasic regional myocardial inflow and outflow: comparison of theory and experiments. *Am J Physiol Heart Circ Physiol* 258: H1687–H1698, 1990.
6. **Chilian WM, Layne SM, Klausner EC, Eastham CL, Marcus ML.** Redistribution of coronary microvascular resistance produced by dipyridamole. *Am J Physiol Heart Circ Physiol* 256: H383–H390, 1989.
7. **Doucette JW, Corl PD, Payne HM, Flynn AE, Goto M, Nassi M, Segal J.** Validation of a Doppler guide wire for intravascular measurement of coronary artery flow velocity. *Circulation* 85: 1899–1911, 1992.
8. **Downey JM, Kirk ES.** Inhibition of coronary blood flow by a vascular waterfall mechanism. *Circ Res* 36: 753–760, 1975.
9. **Garcia D, Barenbrug PJ, Pibarot P, Dekker AL, van der Veen FH, Maessen JG, Dumesnil JG, Durand LG.** A ventricular-vascular coupling model in presence of aortic stenosis. *Am J Physiol Heart Circ Physiol* 288: H1874–H1884, 2005.
10. **Garcia D, Durand LG.** Modeling of aortic stenosis and systemic hypertension. In: *Wiley Encyclopedia of Biomedical Engineering*, edited by Akay M. New York: Wiley, 2006.
11. **Garcia D, Kadem L, Savery D, Pibarot P, Durand LG.** Analytical modeling of the instantaneous maximal transvalvular pressure gradient in aortic stenosis. *J Biomech* 39: 3036–3044, 2006.
12. **Gould KL, Carabello BA.** Why angina in aortic stenosis with normal coronary arteriograms? *Circulation* 107: 3121–3123, 2003.
13. **Heineman FW, Grayson J.** Transmural distribution of intramyocardial pressure measured by micropipette technique. *Am J Physiol Heart Circ Physiol* 249: H1216–H1223, 1985.
14. **Hildick-Smith DJ, Shapiro LM.** Coronary flow reserve improves after aortic valve replacement for aortic stenosis: an adenosine transthoracic echocardiography study. *J Am Coll Cardiol* 36: 1889–1896, 2000.
15. **Hoffman JI.** Problems of coronary flow reserve. *Ann Biomed Eng* 28: 884–896, 2000.
16. **Hoffman JI, Spaan JA.** Pressure-flow relations in coronary circulation. *Physiol Rev* 70: 331–390, 1990.
17. **Holenstein R, Nerem RM.** Parametric analysis of flow in the intramyocardial circulation. *Ann Biomed Eng* 18: 347–365, 1990.
18. **Hongo M, Goto T, Watanabe N, Nakatsuka T, Tanaka M, Kinoshita O, Yamada H, Okubo S, Sekiguchi M.** Relation of phasic coronary flow velocity profile to clinical and hemodynamic characteristics of patients with aortic valve disease. *Circulation* 88: 953–960, 1993.
19. **Hozumi T, Yoshida K, Ogata Y, Akasaka T, Asami Y, Takagi T, Morioka S.** Noninvasive assessment of significant left anterior descending coronary artery stenosis by coronary flow velocity reserve with transthoracic color Doppler echocardiography. *Circulation* 97: 1557–1562, 1998.
20. **Judd RM, Mates RE.** Coronary input impedance is constant during systole and diastole. *Am J Physiol Heart Circ Physiol* 260: H1841–H1851, 1991.
21. **Julius BK, Spillmann M, Vassalli G, Villari B, Eberli FR, Hess OM.** Angina pectoris in patients with aortic stenosis and normal coronary arteries. Mechanisms and pathophysiological concepts. *Circulation* 95: 892–898, 1997.
22. **Kajiya F, Matsuoka S, Ogasawara Y, Hiramatsu O, Kanazawa S, Wada Y, Tadaoka S, Tsujioka K, Fujiwara T, Zamir M.** Velocity profiles and phasic flow patterns in the non-stenotic human left anterior descending coronary artery during cardiac surgery. *Cardiovasc Res* 27: 845–850, 1993.
23. **Kaufmann PA, Camici PG.** Myocardial blood flow measurement by PET: technical aspects and clinical applications. *J Nucl Med* 46: 75–88, 2005.
24. **Kenny A, Wisbey CR, Shapiro LM.** Profiles of coronary blood flow velocity in patients with aortic stenosis and the effect of valve replace-

ment: a transthoracic echocardiographic study. *Br Heart J* 71: 57–62, 1994.
25. **Khouri EM, Gregg DE, Rayford CR.** Effect of exercise on cardiac output, left coronary flow and myocardial metabolism in the unanesthetized dog. *Circ Res* 17: 427–437, 1965.
26. **Krams R, Sipkema P, Westerhof N.** Varying elastance concept may explain coronary systolic flow impediment. *Am J Physiol Heart Circ Physiol* 257: H1471–H1479, 1989.
27. **Lester SJ, Heilbron B, Gin K, Dodek A, Jue J.** The natural history and rate of progression of aortic stenosis. *Chest* 113: 1109–1114, 1998.
28. **Loudon C, Tordesillas A.** The use of the dimensionless Womersley number to characterize the unsteady nature of internal flow. *J Theor Biol* 191: 63–78, 1998.
29. **Mihaljevic T, Nowicki ER, Rajeswaran J, Blackstone EH, Lagazzi L, Thomas J, Lytle BW, Cosgrove DM.** Survival after valve replacement for aortic stenosis: implications for decision making. *J Thorac Cardiovasc Surg* 135: 1270–1278, 2008.
30. **Monrad ES, Hess OM, Murakami T, Nonogi H, Corin WJ, Krayenbuehl HP.** Time course of regression of left ventricular hypertrophy after aortic valve replacement. *Circulation* 77: 1345–1355, 1988.
31. **Nanto S, Masuyama T, Takano Y, Hori M, Nagata S.** Determination of coronary zero flow pressure by analysis of the baseline pressure-flow relationship in humans. *Jpn Circ J* 65: 793–796, 2001.
32. **Petropoulakis PN, Kyriakidis MK, Tentolouris CA, Kourouclis CV, Toutouzas PK.** Changes in phasic coronary blood flow velocity profile in relation to changes in hemodynamic parameters during stress in patients with aortic valve stenosis. *Circulation* 92: 1437–1447, 1995.
33. **Rajappan K, Rimoldi OE, Camici PG, Bellenger NG, Pennell DJ, Sheridan DJ.** Functional changes in coronary microcirculation after valve replacement in patients with aortic stenosis. *Circulation* 107: 3170–3175, 2003.
34. **Rajappan K, Rimoldi OE, Dutka DP, Ariff B, Pennell DJ, Sheridan DJ, Camici PG.** Mechanisms of coronary microcirculatory dysfunction in patients with aortic stenosis and angiographically normal coronary arteries. *Circulation* 105: 470–476, 2002.
35. **Rigo F.** Coronary flow reserve in stress-echo lab. From pathophysiologic toy to diagnostic tool. *Cardiovasc Ultrasound* 3: 8, 2005.
36. **Saltelli A, Ratto M, Andres T, Campolongo F, Cariboni J, Gatelli D, Saisana M, Tarantola S.** *Global Sensitivity Analysis: the Primer*. Chichester, UK: Wiley, 2008.
37. **Schwartzkopff B, Frenzel H, Dieckerhoff J, Betz P, Flasshove M, Schulte HD, Mundhenke M, Motz W, Strauer BE.** Morphometric investigation of human myocardium in arterial hypertension and valvular aortic stenosis. *Eur Heart J* 13, *Suppl.* D: 17–23, 1992.
38. **Schwitter J, Eberli FR, Ritter M, Turina M, Krayenbuehl HP.** Myocardial oxygen consumption in aortic valve disease with and without left ventricular dysfunction. *Br Heart J* 67: 161–169, 1992.
39. **Senzaki H, Chen CH, Kass DA.** Single-beat estimation of end-systolic pressure-volume relation in humans. A new method with the potential for noninvasive application. *Circulation* 94: 2497–2506, 1996.
40. **Smith NP.** A computational study of the interaction between coronary blood flow and myocardial mechanics. *Physiol Meas* 25: 863–877, 2004.
41. **Smith NP, Kassab GS.** Analysis of coronary blood flow interaction with myocardial mechanics based on anatomical models. *Philos Trans R Soc Lond A Math Phys Sci* 359: 1251–1262, 2001.
42. **Sobol IM.** Global sensitivity indices for nonlinear mathematical models and their Monte Carlo estimates. *Math Comput Simul* 55: 271–280, 2001.
43. **Spaan JA, Breuls NP, Laird JD.** Diastolic-systolic coronary flow differences are caused by intramyocardial pump action in the anesthetized dog. *Circ Res* 49: 584–593, 1981.
44. **Stein PD, Marzilli M, Sabbah HN, Lee T.** Systolic and diastolic pressure gradients within the left ventricular wall. *Am J Physiol Heart Circ Physiol* 238: H625–H630, 1980.
45. **Suga H.** Ventricular energetics. *Physiol Rev* 70: 247–277, 1990.
46. **Suga H, Yasumura Y, Nozawa T, Futaki S, Igarashi Y, Goto Y.** Prospective prediction of O_2 consumption from pressure-volume area in dog hearts. *Am J Physiol Heart Circ Physiol* 252: H1258–H1264, 1987.
47. **Sun Y, Gewirtz H.** Estimation of intramyocardial pressure and coronary blood flow distribution. *Am J Physiol Heart Circ Physiol* 255: H664–H672, 1988.
48. **Sung HW, Yu PS, Hsu CH, Hsu JC.** Can cardiac catheterization accurately assess the severity of aortic stenosis? An in vitro pulsatile flow study. *Ann Biomed Eng* 25: 896–905, 1997.
49. **Ting CT, Chen JW, Chang MS, Yin FC.** Arterial hemodynamics in human hypertension. Effects of the calcium channel antagonist nifedipine. *Hypertension* 25: 1326–1332, 1995.
50. **Voudris V, Avramides D, Gatzov P, Malakos J, Skoularigis J, Manolis A, Gavras H, Gavras I, Cokkinos DV.** The effect of rapid decreases of blood pressure by different mechanisms on coronary flow and flow reserve in normal coronary arteries. *Am J Hypertens* 16: 1000–1005, 2003.
51. **Yoshikawa J, Akasaka T, Yoshida K, Takagi T.** Systolic coronary flow reversal and abnormal diastolic flow patterns in patients with aortic stenosis: assessment with an intracoronary Doppler catheter. *J Am Soc Echocardiogr* 6: 516–524, 1993.